





OPEN Cannabidiol mitigates high-fat-diet-induced early-stage inflammation in two adipose tissue fat depots of Wistar rats

Karolina Konstantynowicz-Nowicka¹  , Klaudia Berk², Katarzyna Hodun¹, Algirdas Utkus³, Ewa Harasim-Symor¹ & Adrian Chabowski¹

Cannabidiol (CBD) has potential for treating obesity-induced inflammation; thus, we studied the influence of CBD on the accumulation of lipid precursors of inflammation, the, enzymes, and cytokine levels in the subcutaneous (SAT) and visceral adipose tissue (VAT) of animals with obesity-induced early-stage inflammation. Our experiment was performed on rats fed a high-fat (HFD) or control diet, which received CBD or its vehicle. The accumulation and composition of lipid fractions were assessed via gas–liquid chromatography, whereas the expression of inflammatory pathway enzymes and the cytokine content were evaluated via Western blot or multiplexing, respectively. In addition to selective changes in the content of cytokines, the administration of CBD to HFD-fed rats also decreased the deposition of all the lipid fractions in VAT, whereas in SAT, only the free fatty acid and diacylglycerol fractions were affected. Moreover, CBD reduced the deposition of arachidonic acid and the expression of enzymes associated with the synthesis of lipid precursors of inflammation in both the SAT and VAT of HFD-fed rats. Although the data revealed the beneficial influence of CBD on lipid precursors of inflammation metabolism in both fat depots, more pronounced changes were observed in VAT, which is a tissue that is more predisposed to metabolic disease development.

Keywords Adipose tissue, Cannabidiol, Inflammation, Arachidonic acid, Phytocannabinoids, Obesity

Currently, an unhealthy diet and irregular physical activity promote caloric surplus, where energy is stored as triacylglycerols (TAGs) in subcutaneous (SAT) and visceral (VAT) adipose tissue. Excess adipose tissue mass leads to increases in fat cell size (hypertrophy) and number (hyperplasia), accompanied by chronic low-grade inflammation¹. These alterations are closely related to metabolic disorders, such as insulin resistance, type 2 diabetes, and cardiovascular diseases^{2,3}. Despite the wealth of research in animal and human models, the precise triggers of obesity-induced inflammation in adipose tissue remain elusive, although several initiating processes have been suggested⁴. One theory assumes that chronic adipose hypertrophy promotes hypoxia, intracellular oxidative stress, and necrosis, which, in turn, increase the production of various inflammatory mediators, including interleukin 6 (IL-6), tumor necrosis factor-alpha (TNF- α), and monocyte chemoattractant protein (MCP-1), and attract proinflammatory macrophages and other immune cells. All of these factors ultimately result in fibrosis of dysfunctional adipose tissue, increased ectopic fat storage, and the development of insulin resistance⁵.

The chronic low-grade inflammatory state in adipocytes is also a consequence of increased production of proinflammatory lipid mediators derived from arachidonic acid (AA, C20:4), the dietary supply of which is noticeably increased in overnutrition, especially in high-fat feeding. AA is an essential n-6 polyunsaturated fatty acid (PUFA) and serves as a precursor to the eicosanoid family of bioactive compounds that control immune and inflammatory responses in the body⁶. There is considerable evidence that excessive formation of these AA derivatives, i.e., prostaglandins, leukotrienes, and thromboxane A2 in adipocytes, may escalate their metabolic dysregulation through overreactive inflammatory signaling^{7,8}.

¹Department of Physiology, Medical University of Białystok, Mickiewicz Str. 2 C, Białystok 15-222, Poland. ²Head and Neck Surgery Clinic for Children and Young Adults, Department of Clinical Pediatrics, Voivodeship Specialist Children's Hospital, Żołnierska Str. 18a, Olsztyn 10-561, Poland. ³Department of Human and Medical Genetics, Institute of Biomedical Sciences, Faculty of Medicine, Vilnius University, Santariškių Str. 2, Vilnius LT-08661, Lithuania. ✉email: karolina.konstantynowicz-nowicka@umb.edu.pl

Currently, the correlations among obesity, adipose tissue inflammation, and metabolic disease make inflammatory pathways attractive targets for the treatment of metabolic diseases. However, the clinical efficacy of drugs targeting these pathways has been disappointing, and new therapeutic alternatives are constantly being explored³. At present, much attention is being given to *Cannabis sativa* components due to their beneficial metabolic properties, which are proposed for use in the treatment of obesity.

CBD is a non-psychotomimetic cannabinoid obtained from medicinal and fiber-type *Cannabis sativa* L. plants⁹. The pharmacokinetics of CBD and the effects observed depend on the formulation and route of administration¹⁰. CBD is well known for its antipsychotic, anxiolytic, sedative, antiepileptic, and analgesic properties^{11,12}. Moreover, it is among the best-explored phytocannabinoids that positively affect lipid and glucose metabolism in different tissues¹³. In adipose tissue, Silvestri et al. reported that CBD dose- and time-dependently reduced intracellular TAG accumulation in oleic acid-treated 3T3-L1 adipocytes¹⁴. In addition, an in vitro study of 3T3-L1 adipocytes revealed that CBD exerts its antiobesity effect through an increase in oxygen consumption and activation of the beta-adrenergic signaling pathway, resulting in lower levels of intracellular fat accumulation¹³. Nevertheless, the exact mechanism of CBD action, which induces metabolic changes in adipocytes, is still poorly defined. Notably, CBD is the most valuable pharmaceutical since it has been found to possess high antioxidant and anti-inflammatory activities^{15,16}. However, until now, it has not been entirely clear whether its action also involves adipose tissue in an overnutrition state. Numerous preclinical reports have demonstrated the tissue-protective and anti-inflammatory effects of CBD in models of neurodegeneration/neuroinflammation, arthritis, primary diabetes, diabetic complications, or cancer^{17,18}. Thus, we speculated that CBD could be effective in reducing obesity-associated inflammation. In the present study, we aimed to investigate the impact of CBD on lipid precursors involved in inflammation, the enzymes of the inflammatory pathway, and selected cytokine levels in the SAT and VAT of rats with obesity induced by a high-fat diet (HFD).

Materials and methods

Animal model and experimental protocol

The entire study involved 40 male Wistar rats weighing between 70 and 100 g before the beginning of the experiment. The rats were obtained and housed in the Experimental Medicine Centre at the Medical University of Bialystok in standard laboratory facilities, which included a reversed 12-hour light-dark cycle, a temperature of 22 ± 2 °C, a plastic autoclave, individually ventilated cages, unlimited access to water and suitable chow. After a week of adaptation to the holding conditions, the rats were allocated into four experimental groups (Fig. 1) via a randomization method that included online random number generators. The control and CBD groups, with ten rats in each, were given a standard diet for rodents (Labofeed B, Kcynia, Poland), which contained 62% carbohydrates, 22% protein, and 16% fat and fatty acid composition described by Nowacki et al.¹⁹. In contrast, the HFD and HFD + CBD groups, with ten rats in each, received a high-fat diet (Research Diets, New Brunswick, NJ, USA, cat. no. D12492) that was composed of 59% fat, 21% protein, and 20% carbohydrates with a fatty acid composition available in the literature²⁰. The feeding period lasted for 7 weeks, and during the last 14 days of the experiment, the animals received simultaneously a selected diet and cannabidiol (CBD) (THC Pharm GmbH, Frankfurt, Germany) or its solvent. CBD was administered intraperitoneally at a dose of 10 mg/kg body weight once a day at the same time in the CBD and HFD + CBD groups in a volume of 1 ml/kg body weight. The CBD dose was selected on the basis of the available literature because it is the most effective²¹. Moreover, the intraperitoneal route of administration was selected even though oral CBD administration is more common in

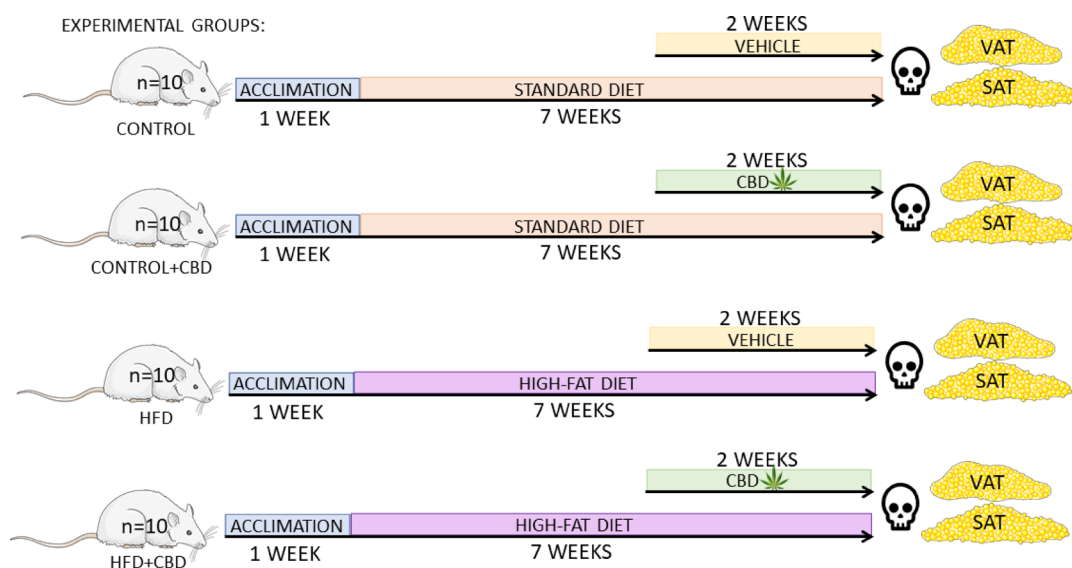


Fig. 1. The experimental design scheme. The description of every experimental group is provided in the *Animal Model and Experimental Protocol* section. The figure was created with the use of Server Medical Art (<https://smart.servier.com>), licensed under CC BY 4.0 (<https://creativecommons.org/licenses/by/4.0/>).

the literature. Some studies have shown that oral CBD administration resulted in the formation of psychoactive CBD derivatives when exposed to a gastric acidic environment, and such psychoactive metabolites were also present in the brain^{22,23}. However, in human and in vivo studies such conversion did not occur and the possibility of psychoactive CBD derivatives formation depends more from purity of CBD, which was high ($\geq 99\%$) used in the present study²⁴. In addition, intraperitoneal route of administration offers practical advantages like reduced procedural stress, lower risk of injury compared with oral savage, and potentially lower intra-day and inter-animal variability. The CBD solvent consisted of 3:1:16, 70% ethanol:2% Tween-80:0.9% NaCl, and it was also administered to the control and HFD groups without CBD in the same volume of 1 ml/kg of body weight. The final CBD solution was prepared from a stock solution where CBD was solubilized in 70% ethanol at 37 °C with gentle shaking immediately before use and protected from light. The amount of CBD administered was calculated on the basis of the current body mass of the rats, and the animal weight was monitored throughout the study. The results depicting increased body weight after HFD and a lack of changes after CBD treatment were shown in our previous work²⁵. At the end of our experiment and 24 h after the last CBD or vehicle dose was applied, the rats were sedated via isoflurane inhalation. The samples of SAT (inguinal) and VAT (epididymal) were taken from sedated animals and immediately frozen in liquid nitrogen with precooled tongs. The collected adipose tissue samples were stored at -80 °C until use. All the experimental protocols were carried out in accordance with the relevant guidelines and regulations. The animal experiments adhered to the ARRIVE guidelines and were approved by the Animal Ethics Committee in Olsztyn (Approval No. 71/2018).

Analysis of tissue lipid contents

Using a mixture of chloroform and methanol at a ratio of 2:1, lipids were extracted from VAT and SAT samples following the procedure detailed precisely in our earlier work²⁶, which was based on Folch et al.²⁷, with slight modifications. An internal standard consisting of heptadecanoic, diheptadecanoic, and triheptadecanoic acids was added to the tubes containing the obtained extracts. Next, via thin-layer chromatography (TLC), the extracts were separated into certain lipid fractions, including diacylglycerols (DAGs), triacylglycerols (TAGs), free fatty acids (FFAs), and phospholipids (PLs), in separation buffer on glass chromatographic plates coated with silica gel (Silica Plate 60, 0.25 mm; Merck, Darmstadt, Germany). After separation, the lipid fractions were then transmethylated with the use of 14% boron trifluoride in methanol and subsequently dissolved in hexane. On the basis of the retention times of the standards, the fatty acid methyl esters in the abovementioned lipid fractions were assessed via gas-liquid chromatography (GLC, Hewlett-Packard 5890 Series II Gas Chromatograph, Agilent Technologies, Santa Clara, CA, USA) equipped with a capillary column (Hewlett-Packard-INNOWax) and flame ionization detector, as previously described by Chabowski et al.²⁸. The total lipid concentration (FFA, DAG, TAG, and PL) in adipose tissue was calculated as the sum of individual fatty acid concentrations in the chosen fraction. The concentrations of the total lipid fractions and arachidonic acid (AA) content are presented in nanomoles per gram of tissue. Moreover, depending on the fatty acid composition, the activities of the n-3 (20:5 + 22:6)/18:3 and n-6 (20:4/18:2 n-6) pathways in a particular lipid fraction were estimated.

Analysis of protein expression

The expression of proteins involved in the synthesis pathways of eicosanoids and prostanoids was determined via Western blot (WB) analysis according to the comprehensive protocol outlined in our previous work²⁹. In the first step, the adipose tissue samples were homogenized via radioimmunoprecipitation assay (RIPA) buffer that included inhibitors of phosphatases and proteases (Roche, Mannheim, Germany). To assess the total protein concentration in the homogenates, a bicinchoninic acid (BCA) assay was performed with bovine serum albumin used as a standard. After the reconstitution of the tissue homogenates in Laemmli buffer (Bio-Rad, Hercules, CA, USA), an equivalent volume of protein was loaded on Criterion TGX Stain-Free Precast Gels (Bio-Rad; Hercules, CA, USA). The proteins separated via electrophoresis were transferred onto nitrocellulose or PVDF membranes. Next, the membranes were subjected to a blocking step with Tris-buffered saline buffer containing Tween-20 (TBST) and either 5% nonfat dry milk or 5% BSA and subsequently immunoblotted overnight with the following primary antibodies of interest: 5-lipoxygenase (5-LOX, 1:1500; Abcam, Cambridge, UK), 12/15-lipoxygenase (12/15-LOX, 1:500; Santa Cruz Biotechnology, Inc., Dallas, TX, USA), cyclooxygenase-1 (COX-1, 1:500; Santa Cruz Biotechnology, Inc., Dallas, TX, USA), and cyclooxygenase-2 (COX-2, 1:500; Santa Cruz Biotechnology, Inc., Dallas, TX, USA). Thereafter, the nitrocellulose membranes were treated with the corresponding horseradish peroxidase (HRP)-conjugated antibodies. The protein bands were detected via a chemiluminescence substrate (Clarity Western ECL Substrate; Bio-Rad, Hercules, CA, USA), and the immunoblotting signals were analyzed via a densitometric visualization system (ChemiDoc, Image Laboratory Software; Bio-Rad, Warsaw, Poland). The standardization process involved overlapping the images of the obtained protein and the total protein after membrane transfer in the ImageLab system (Bio-Rad, Warsaw, Poland), with the control group designated 100%.

Analysis of cytokine and chemokine contents

A commercially available multiplex assay kit (Bio-Plex Immunoassay Kit, Bio-Plex Pro Rat Cytokine 23-Plex Assay, Bio-Rad; Warsaw, Poland) was used to assess the contents of selected cytokines and chemokines, namely, interleukin 18 (IL-18), interleukin 17 A (IL-17 A), interleukin 13 (IL-13), interleukin 12 p70 (IL-12 p70), interleukin 10 (IL-10), interleukin 7 (IL-7), interleukin 6 (IL-6), interleukin 5 (IL-5), interleukin 4 (IL-4), interleukin 2 (IL-2), interleukin 1 β (IL-1 β), interleukin 1 α (IL-1 α), interferon γ (IFN- γ), regulated on activation normal T-cell expressed and secreted (RANTES), tumor necrosis factor α (TNF- α), macrophage inflammatory protein 3 α (MIP-3 α), macrophage inflammatory protein 1 α (MIP-1 α), granulocyte-macrophage colony-stimulating factor (GM-CSF), granulocyte colony-stimulating factor (G-CSF), growth-regulated oncogenes/keratinocyte chemoattractant (GRO/KC), and vascular endothelial growth factor (VEGF), as described previously²⁶.

In accordance with the manufacturer's protocol, before the multiplex assay procedure, the SAT and VAT homogenates were centrifuged twice (at $15,000 \times g$ for 10 min at 4°C), and the concentration of total protein in the obtained supernatants was estimated via the BCA method described previously in the Western blot section. Next, the supernatants, where the total protein concentration ranged between 500 and $900 \mu\text{g/ml}$, were collected in new tubes and stored at -80°C until further use. In the first step, the diluted Bio-Plex Wash Buffer mixture of beads was placed in each well of a whole 96-well assay plate, and then, the same wash buffer was used to wash the plate two times. Next, $50 \mu\text{l}$ of vortexed blanks, standards, or samples were added to particular wells and incubated at room temperature for 1 h. After a series of consecutive washes, the detection antibodies contained in the kit were added to each well, and a 30 min incubation was conducted. After three washes, streptavidin-phycoerythrin (SA-PE) solution was added to each well and incubated for 10 min. After the next three washes, the resuspended magnetic beads were applied, and the plate was shaken for 30 s. As the last step of the procedure, the Bio-Plex 200 system (Bio-Rad Laboratories, Inc.; Hercules, CA, USA) connected with Bio-Plex Manager Software was used to read the plate. The concentrations of selected cytokines and chemokines were assessed via individual standard curves created for each analyte and are presented in picograms per milliliter of protein.

Histological analysis

First, the samples of SAT and VAT isolated from dormant animals were fixed in 10% buffered formalin and embedded in paraffin blocks, which were cut into $4 \mu\text{m}$ -thick sections and attached to glass slides (Superfrost Plus; Menzel Gläser, Braunschweig, Germany). Next, the sections were deparaffinized and hydrated in pure alcohol. For general histological evaluation, the sections were stained with eosin and briefly rinsed in 50% ethanol followed by tap water, and the nuclei were stained with Mayer's hematoxylin for 2 min. After rising in tap water, the sections were mounted in glycerine jelly. Finally, the results of the staining (five randomly selected microscopic fields of 0.785 mm^2 from SAT and VAT) were evaluated under an Olympus BX41 light microscope with an Olympus DP12 camera under a magnification of $200\times$ ($20\times$ lens and $10\times$ eyepiece) equipped with Olympus CellSens Imaging Software Version 3.1. Each obtained digital image was subjected to morphometric evaluation via NIS Elements AR 3.10 Nikon software for microscopy image analysis. In each analyzed image, the circumference of adipocytes was measured in both SAT and VAT in all experimental groups. Approximately 20 adipocytes were assessed per image, and nearly all cells visible within the examined field were included in the analysis. The results were plotted in GraphPad Prism 8 (GraphPad Software, La Jolla, CA, USA). The data are presented as the means \pm standard deviations; $p < 0.05$.

Statistical analysis

The results are expressed as the mean values \pm standard deviations (SD) and are derived from ten (GLC, multiplex) or six (Western blot) separate determinations across all the groups. Bartlett's test and the Shapiro-Wilk test were performed to evaluate the homogeneity of the variance and the normality of the data distribution, respectively. The statistical assessment was conducted via two-way ANOVA followed by the respective post hoc test via GraphPad Prism 8.2.1 (GraphPad Software, San Diego, CA, USA). The differences were considered statistically significant at $p < 0.05$. In the statistical analysis, no correction for multiple comparisons was applied; if so, the significance threshold would be a p value less than 0.01250 when the Bonferroni correction was used.

Results

Effect of CBD treatment on the contents of lipid fractions in the SAT and VAT

SAT

In our study, we observed a substantial increase in the FFA level ($+27.3\%$, $p = 0.0017$; Fig. 2A) in the SAT in the HFD group compared with that in the control group. Concomitantly, we revealed a decreased content of FFAs (-23.9% , $p = 0.0005$; Fig. 2A) in the HFD + CBD group compared with the appropriate HFD group. Furthermore, the DAG content in the HFD group was greater ($+45.6\%$, $p = 0.0039$; Fig. 2B) than that in the proper control group. Compared with the corresponding HFD group, the HFD group treated with CBD presented a significant reduction in the DAG concentration (-22.0% , $p = 0.0185$; Fig. 2B). We noticed an elevated content of PL in both HFD groups (HFD: $+41.4\%$, $p = 0.0068$; HFD + CBD: $+69.5\%$, $p = 0.0015$; Fig. 2D) compared with the appropriate control group.

VAT

In VAT, the FFA concentration in the HFD + CBD group was lower than that in the appropriate control group or in the HFD group (-48.7% , $p < 0.0001$, vs. the control group; -52.5% , $p < 0.0001$, vs. the HFD group; Fig. 2A). Moreover, the DAG concentration in the HFD group was greater ($+80.0\%$, $p < 0.0001$; Fig. 2B) than that in the corresponding control group. Compared with the proper HFD group, the HFD-induced obesity group treated with CBD presented a marked reduction in the content of DAG (-49.8% , $p < 0.0001$; Fig. 2B). In the HFD group, we also demonstrated an increase in the level of TAG ($+43.4\%$, $p < 0.0001$; Fig. 2C) compared with that in the proper control group. Compared with HFD alone, two-week CBD administration resulted in a considerable decrease in the level of TAG (-27.7% , $p = 0.0002$; Fig. 2C). In the HFD-induced obesity group, we also observed an increase in the content of PL ($+48.8\%$, $p = 0.0001$; Fig. 2D) compared with that in the corresponding control group. Similarly, in the HFD + CBD group, the content of PL was lower (-41.2% , $p = 0.0185$; Fig. 2D) than that in the proper HFD group.

The activity of the n-3 pathway in the FFA, DAG, TAG, and PL fractions

SAT

In the SAT, we demonstrated an increase in n-3 pathway activity in the FFA and DAG fractions in the CBD group ($+42.2\%$, $p = 0.0135$, $+31.4\%$, $p = 0.0068$; Fig. 3A and B) compared with the proper control group. Compared

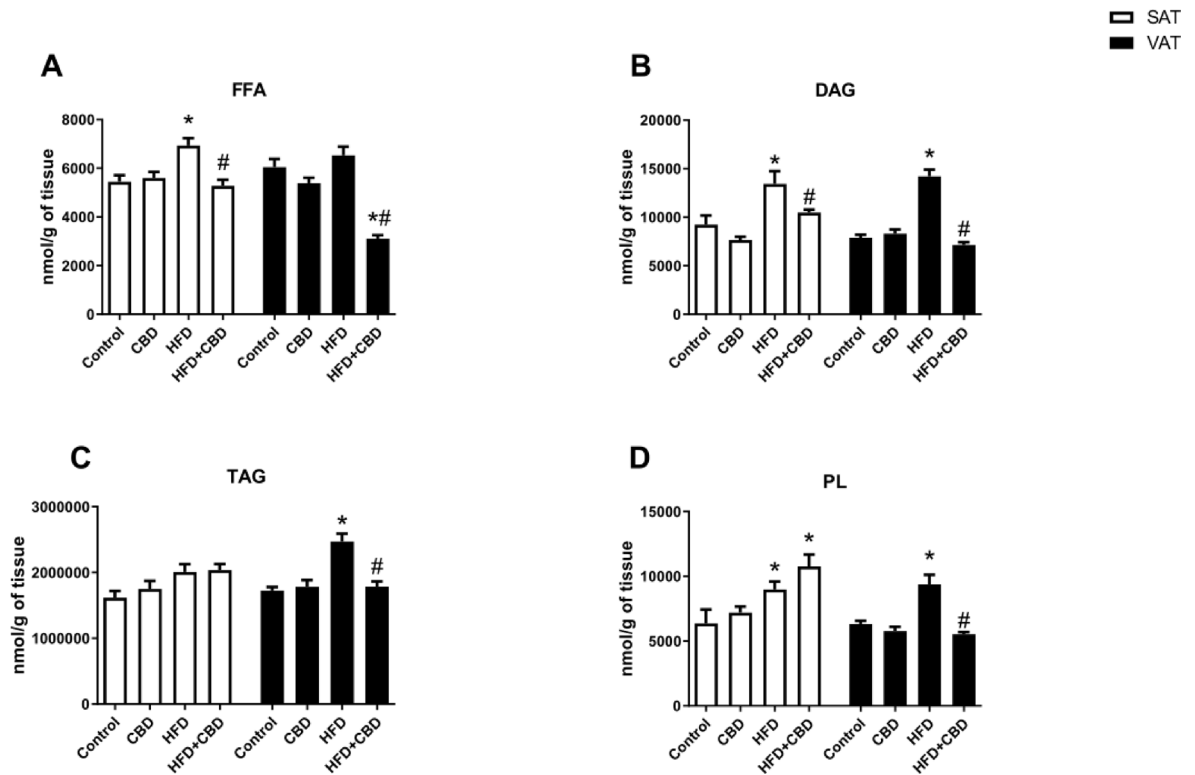


Fig. 2. Concentrations of (A) free fatty acid (FFA), (B) diacylglycerol (DAG), (C) triacylglycerol (TAG), and (D) phospholipid (PL) fractions after two weeks of treatment with cannabidiol (CBD) in the SAT and VAT of rats fed a standard diet (Control) or high-fat diet (HFD). The data are presented as the mean values \pm SD, $n = 10$ in each group. * $p < 0.05$, significant difference: control group vs. experimental group; # $p < 0.05$, significant difference: HFD vs. experimental group.

with that in the control group, the activity of the n-3 pathway in the TAG fraction was decreased in both the HFD and HFD + CBD groups (HFD: -46.0% , $p < 0.0001$; HFD + CBD: -56.7% , $p < 0.0001$; Fig. 3C). Furthermore, the n-3 activity pathway in the PL fraction was greater in the CBD group ($+39.6\%$, $p = 0.0129$; Fig. 3D) and lower in the HFD + CBD group (-39.7% , $p < 0.0001$; Fig. 3D) than in the control group.

VAT

In the HFD + CBD group, we observed a significant increase in the n-3 activity pathway in the FFA fraction ($+42.3\%$, $p = 0.0039$, vs. the control group; $+42.1\%$, $p = 0.0005$, vs. the HFD group; Fig. 3A). A decrease in the activity of the n-3 pathway in the TAG fraction was observed in each experimental group (CBD: -22.3% , $p = 0.0015$; HFD: -65.9% , $p < 0.0001$; HFD + CBD: -55.7% , $p = 0.0002$; Fig. 3C) compared with the control group. However, the activity of the n-3 pathway was greater in the HFD + CBD group ($+29.7\%$, $p = 0.0012$; Fig. 3C) than in the corresponding HFD group.

Activity of the n-6 pathway in the FFA, DAG, TAG, and PL fractions

SAT

There was a marked decline in the activity of the n-6 pathway in the FFA fraction in the CBD and HFD groups (-33.2% , $p = 0.0001$ – 37.0% , $p = 0.0003$, vs. the control group, respectively; Fig. 4A). A significant increase ($+49.6\%$, $p = 0.0020$, vs. the HFD group; Fig. 4A) in the n-6 activity pathway in the FFA fraction was demonstrated in the HFD + CBD group. In the DAG fraction, we observed an increase in the n-6 activity pathway in the HFD group ($+66.3\%$, $p < 0.0001$, vs. the control group; Fig. 4B). In turn, in the HFD + CBD group, we demonstrated a decrease (-29.6% , $p = 0.0037$; Fig. 4B) in the activity of this pathway compared with that in the HFD group. Compared with that in the control group, the activity of the n-6 pathway in the TAG fraction was lower in the HFD + CBD group (-32.1% , $p < 0.0001$; Fig. 4C). There were significant alterations in the n-6 activity pathway in the HFD group ($+31.6\%$, $p = 0.0269$, vs. the control group; Fig. 4D) and in the HFD + CBD group (-47.7% , $p < 0.0001$, vs. the HFD group; Fig. 4D).

VAT

In our study, the activity of the n-6 pathway in the FFA fraction was lower in the CBD and HFD groups (-38.6% , $p < 0.0001$, -26.7% , $p = 0.0011$, vs. the control group, respectively; Fig. 4A). Concomitantly, in this fraction, we noticed greater activity in the n-6 pathway in the HFD + CBD group ($+55.1\%$, $p = 0.0004$, vs. the control group; $+111.5\%$, $p < 0.0001$, vs. the HFD group; Fig. 4A). There were also changes in the activity of the n-6 pathway

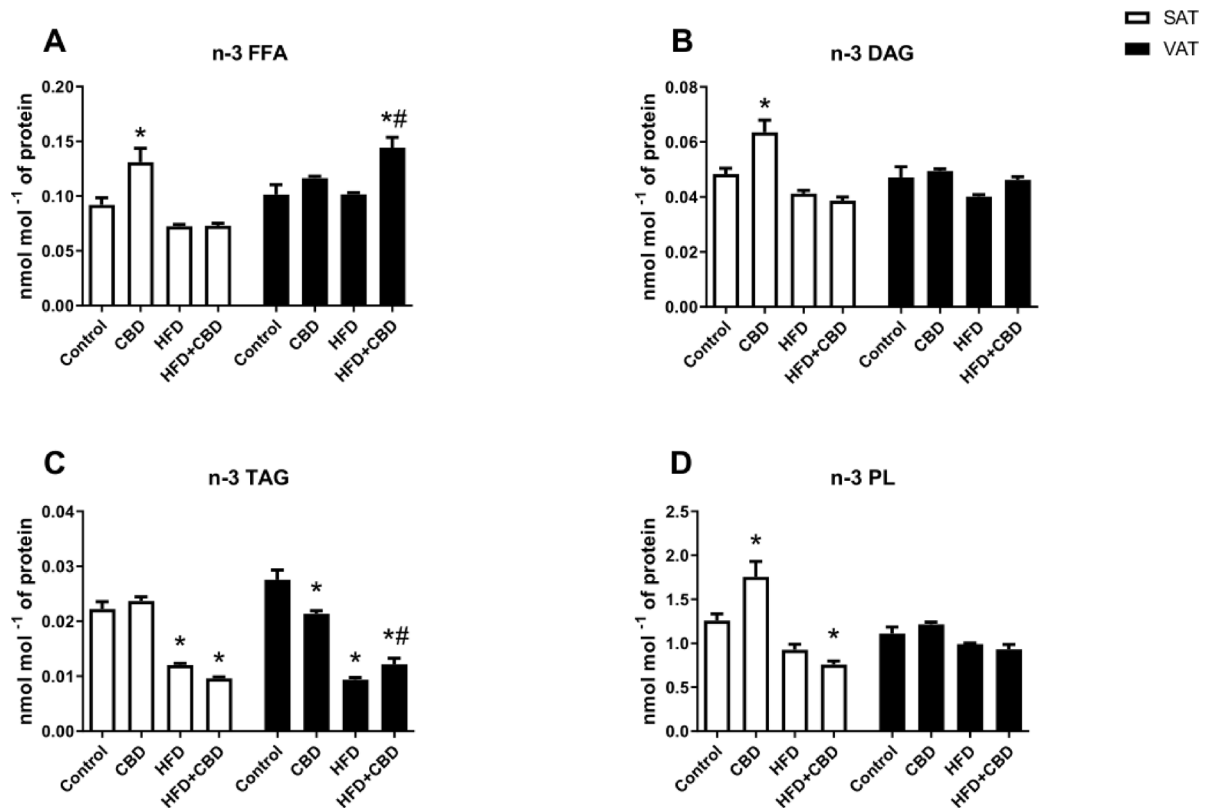


Fig. 3. The activity of the n-3 pathway ((20:5 + 22:6)/18:3) in (A) free fatty acid (FFA), (B) diacylglycerol (DAG), (C) triacylglycerol (TAG), and (D) phospholipid (PL) fractions after two-week treatment with cannabidiol (CBD) in the SAT and VAT of rats fed a standard diet (Control) or high-fat diet (HFD). The data are presented as the mean values \pm SD, $n = 10$ in each group. * $p < 0.05$, significant difference: control group vs. experimental group; # $p < 0.05$, significant difference: HFD vs. experimental group.

in the DAG fraction (CBD: -21.4% , $p = 0.0025$; HFD: $+27.3\%$, $p = 0.0184$; Fig. 4B) compared with that in the standard diet group. In the TAG fraction in VAT, the activity of the n-6 pathway was elevated in the HFD group ($+37.0\%$, $p = 0.0067$, vs. the control group; Fig. 4C). In this fraction, there was a significant decrease in the n-6 activity pathway in HFD-induced obese rats treated with CBD (-47.6% , $p < 0.0001$, vs. the control group; -61.7% , $p < 0.0001$, vs. the HFD group; Fig. 4C). In the PL fraction, the activity of the n-6 pathway was elevated in the HFD group ($+31.6\%$, $p = 0.0016$, vs. the control group; Fig. 4D). Additionally, the n-6 activity pathway in the HFD + CBD group was reduced (-33.7% , $p = 0.0006$; Fig. 4D) compared with that in the appropriate HFD group.

Effects of two-week CBD treatment on the concentrations of AA in the SAT and VAT

SAT

In the SAT, in the FFA fraction of the rats subjected to the HFD, we observed a significant increase in the content of AA ($+104.7\%$, $p < 0.0001$; Fig. 5A) compared with that of the rats fed the standard diet. Our study revealed that the concentration of AA in the FFA fraction was lower during the chronic administration of CBD to rats fed a HFD (-23.9% , $p = 0.0017$, vs. the control group; -69.2% , $p < 0.0001$, vs. the HFD group; Fig. 5A). Furthermore, in the DAG fraction, the level of AA significantly decreased in both the CBD and HFD + CBD groups (CBD: -48.6% , $p = 0.0001$, vs. the control group; HFD + CBD: -49.1% , $p = 0.0001$, vs. the control group; -52.6% , $p < 0.0001$, vs. the HFD group; Fig. 5B). The concentration of AA in the TAG fraction was significantly increased in the HFD group ($+18.1\%$, $p = 0.0368$ vs. the Control group; Fig. 5B). Moreover, CBD application to rats fed standard and HFD led to a marked reduction in the AA level in the TAG fraction (CBD: -62.7% , $p < 0.0001$, vs. the control group; HFD + CBD: -67.2% , $p < 0.0001$, vs. the control group, -72.3% , $p < 0.0001$, vs. the HFD group; Fig. 5C). In our study, we observed a significant increase in the tissue level of AA in the PL fraction in the CBD, HFD and HFD + CBD groups (CBD: $+102.8\%$, $p = 0.0002$; HFD: $+168.8\%$, $p = 0.0001$; HFD + CBD: $+19.3\%$, $p = 0.0279$; Fig. 5D) compared with the control group. Furthermore, in the HFD group treated with CBD, the concentration of AA was significantly lower than that in the HFD group (-55.6% , $p < 0.0001$; Fig. 5D).

VAT

In our study, we noted a substantially elevated content of AA in the FFA fraction in the VAT of HFD-fed rats ($+76.1\%$, $p = 0.0003$; Fig. 5A) compared with that in the control group. We also observed a reduction in the level of AA in the FFA fraction after two weeks of CBD treatment in HFD-fed rats (-11.0% , $p = 0.0433$, vs. the control

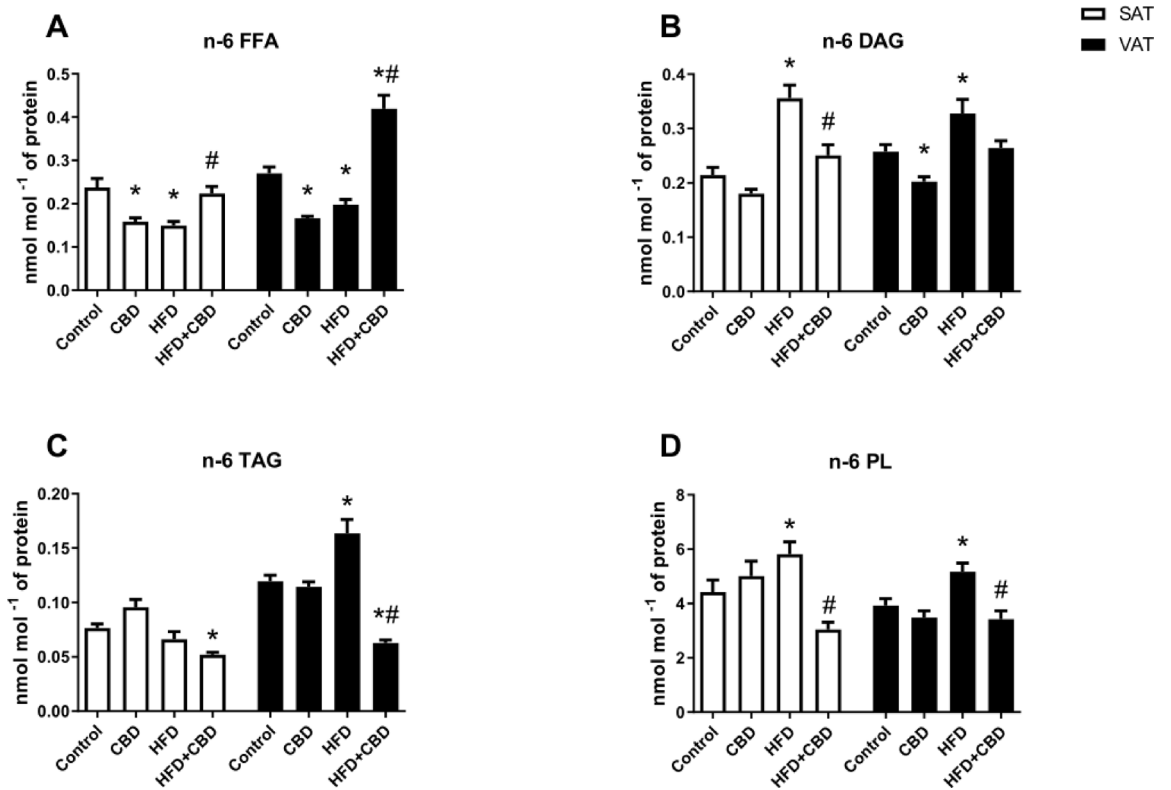


Fig. 4. The activity of the n-6 pathway (20:4/18:2) in (A) free fatty acid (FFA), (B) diacylglycerol (DAG), (C) triacylglycerol (TAG), and (D) phospholipid (PL) fractions after two-week treatment with cannabidiol (CBD) in the SAT and VAT of rats fed a standard diet (Control) or high-fat diet (HFD). The data are presented as the mean values \pm SD, $n = 10$ in each group. * $p < 0.05$, significant difference: control group vs. experimental group; # $p < 0.05$, significant difference: HFD vs. experimental group.

group; -63.7% , $p < 0.0001$; Fig. 5A). In the DAG fraction, the AA content was lower in the CBD and HFD + CBD groups (CBD: -46.5% , $p = 0.0002$, vs. the control group; HFD + CBD: -52.9% , $p < 0.0001$, vs. the control group; -56.5% , $p < 0.0001$, vs. the HFD group; Fig. 5B). Furthermore, in the CBD and HFD + CBD groups, we observed a decrease in the content of AA in the TAG fraction (CBD: -71.1% , $p < 0.0001$; HFD + CBD: -68.3% , $p < 0.0001$ vs. the control group; HFD + CBD: -51.4% , $p < 0.0001$, vs. the HFD group; Fig. 5C) compared with that in the standard and HFD groups. There was also a significant decrease in the AA concentration in the TAG fraction of rats with HFD-induced obesity (-72.3% , $p = 0.0014$; Fig. 5C) compared with that in the control group. In the VAT, we also noticed an increase in the AA content in the PL fraction in the HFD group ($+47.9\%$, $p = 0.0237$; Fig. 5D) compared with that in the control group. Moreover, in the PL fraction, the level of AA significantly decreased in the HFD + CBD group compared with the proper control and HFD groups (-28.1% , $p < 0.0001$, vs. the control group, -51.4% , $p = 0.0009$ vs. the HFD group; Fig. 5D).

Effect of two-week CBD treatment on the expression of proteins from the eicosanoid synthesis pathway in the SAT and VAT

SAT

There was a decrease in COX-1 expression (-49.8% , $p = 0.0016$, vs. the control group; Fig. 6A) during chronic CBD administration in rats fed standard chow. Compared with those in the control group, the total expression of COX-1 in HFD-fed animals was elevated ($+28.3\%$, $p = 0.0132$; Fig. 6A). Moreover, in the HFD + CBD group, we demonstrated a decrease in the expression of COX-1 (-42.0% , $p = 0.0003$; Fig. 6A) compared with that in the HFD group. The expression of COX-2 in the adipose tissue of rats from both the CBD alone and CBD with HFD-treated groups was lower (CBD: -46.4% , $p = 0.0120$; HFD + CBD: -44.6% , $p = 0.0092$; Fig. 6B) than that in the proper control group. In our study, in the HFD group, we observed a marked increase in the expression of COX-2 ($+42.4\%$, $p = 0.0221$; Fig. 6B) compared with that in the control group. Concomitantly, we found a decrease in the expression of COX-2 in the CBD-treated group fed a HFD (-61.1% , $p < 0.0001$; Fig. 6B) compared with the experimental model of HFD-induced obesity. Moreover, we detected a decrease in the expression of 5-LOX in the CBD alone group (-31.6% , $p = 0.0294$; Fig. 6C) compared with that in the control group. Compared with the control, HFD-induced obesity caused elevated expression of 12-/15-LOX ($+150.8\%$, $p < 0.0001$; Fig. 6D). On the other hand, we revealed that CBD administration to HFD-fed rats decreased the expression of 12-/15-LOX (-63.1% , $p = 0.0002$; Fig. 6D) compared with that in the HFD group.

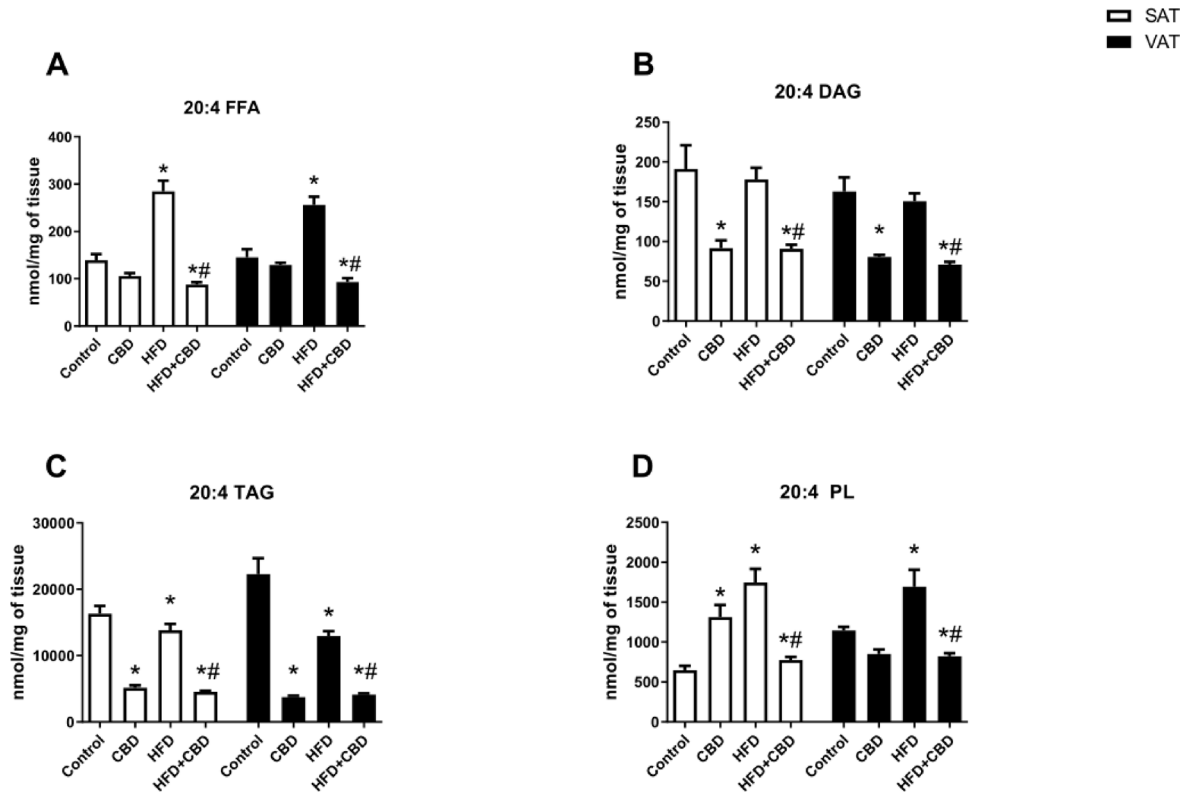


Fig. 5. Concentration of arachidonic acid (20:4) in the (A) free fatty acid (FFA), (B) diacylglycerol (DAG), (C) triacylglycerol (TAG), and (D) phospholipid (PL) fractions after two-week treatment with cannabidiol (CBD) in the SAT and VAT of rats fed a standard diet (Control) or high-fat diet (HFD). The data are presented as the mean values \pm SD, $n = 10$ in each group. * $p < 0.05$, significant difference: control group vs. experimental group; # $p < 0.05$, significant difference: HFD vs. experimental group.

VAT

Compared with that in the appropriate control group, the expression of COX-1 in the CBD group was lower (-41.6% , $p = 0.0183$; Fig. 6A). Interestingly, compared with HFD consumption, CBD administration resulted in a decrease in the total expression of COX-1 (-48.4% , $p = 0.0079$; Fig. 6A). The expression of COX-2 in the CBD-treated HFD group decreased (-26.8% , $p = 0.0216$; Fig. 6B) compared with that in the rats fed the HFD alone. Compared with those in the control group, the total expression of 5-LOX in the HFD-fed group was significantly lower (-36.3% , $p = 0.0161$; Fig. 6C). In addition, we observed an increase in the expression of 12-/15-LOX in the HFD + CBD group ($+35.2\%$, $p = 0.0425$; Fig. 6D) compared with that in the HFD group.

Effects of two-week CBD treatment on the concentrations of lipid cytokines in the SAT and VAT

SAT

Compared with control rats, CBD-treated rats fed a standard diet presented alterations in the concentrations of G-CSF, IFN- γ , M-CSF, and VEGF (-44.0% , $p = 0.0119$; $+54.4\%$, $p = 0.0457$; $+221.2\%$, $p < 0.0001$; $+112.2\%$, $p = 0.0023$, respectively; Table 1). Compared with those in the control group, we detected significant changes in HFD group in the levels of cytokines, namely, G-CSF, IFN- γ , IL-10, IL-13, and TNF- α (-35.9% , $p = 0.0035$; $+89.6\%$, $p = 0.0120$; $+70.3\%$, $p = 0.0074$; -43.4% , $p = 0.0061$; $+76.0\%$, $p = 0.0021$, respectively; Table 1). In turn, in the HFD + CBD group, we observed increases in the content of GM-CSF ($+59.4\%$, $p = 0.0155$, vs. the control group; Table 1), IL-1 α ($+34.3\%$, $p = 0.0245$, vs. the control group; $+48.2\%$, $p = 0.0098$, vs. the HFD group; Table 1), IL-4 ($+68.4\%$, $p = 0.0128$, vs. the control group; $+60.8\%$, $p = 0.0239$, vs. the HFD group; Table 1), IL-12 p70 ($+52.0\%$, $p = 0.0176$, vs. the HFD group; Table 1), MCP-1 ($+70.0\%$, $p = 0.0071$, vs. the control group; Table 1), M-CSF ($+80.6\%$, $p = 0.0062$, vs. the control group; Table 1), and VEGF ($+86.5\%$, $p = 0.0019$, vs. the control group; $+88.4\%$, $p = 0.0017$, vs. the HFD group; Table 1). Additionally, there were significant decreases in the content of G-CSF (-47.0% , $p = 0.0021$, vs. the control group; Table 1), IL-10 (-32.2% , $p = 0.0359$, vs. the HFD group; Table 1), and IL-18 (-60.9% , $p = 0.0002$, vs. the control group; -63.9% , $p = 0.0003$, vs. the HFD group; Table 1) in the CBD-treated rats receiving a HFD.

VAT

In the CBD group, we observed marked changes in the concentrations of IFN- γ ($+81.8\%$, $p = 0.0001$; Table 2), IL-4 ($+72.6\%$, $p = 0.0022$; Table 2), IL-6 ($+77.1\%$, $p = 0.0161$; Table 2), IL-7 (-27.1% , $p = 0.0400$; Table 2), IL-10

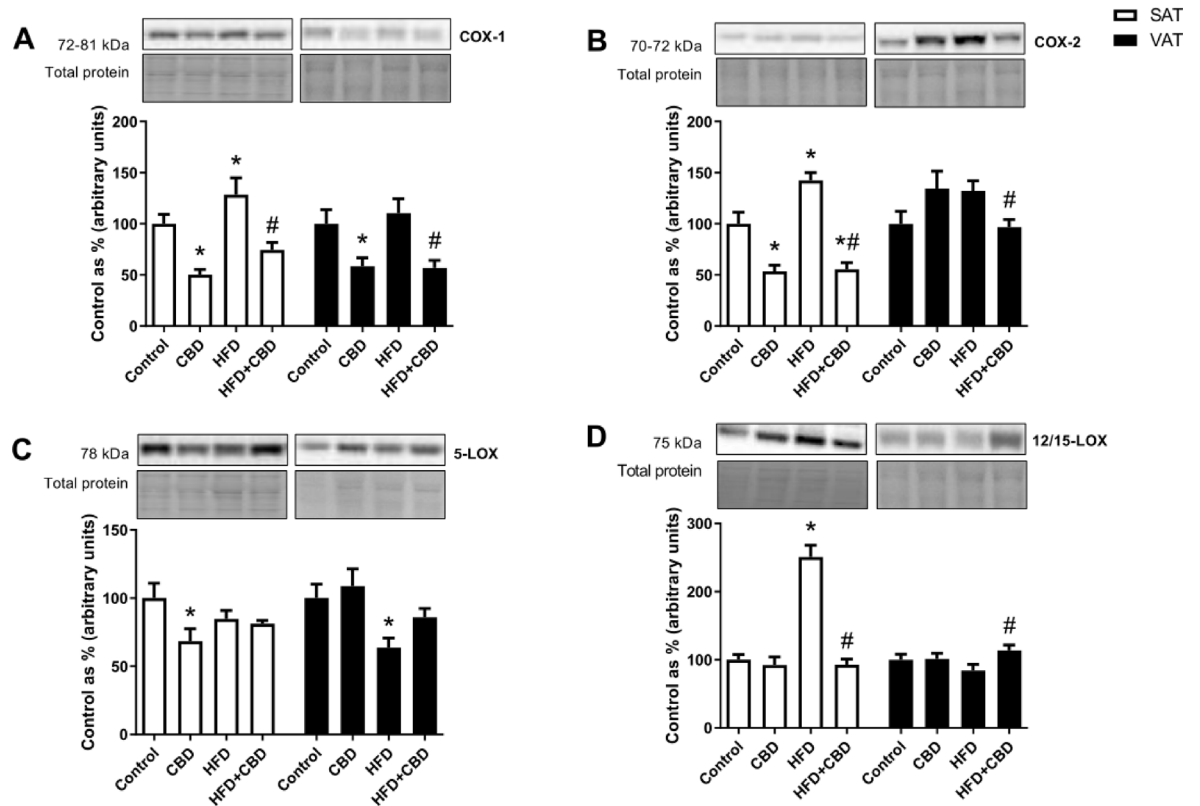


Fig. 6. The expression of proteins from the eicosanoid and prostanoid synthesis pathway: (A) 5-lipoxygenase (5-LOX), (B) 12/15-lipoxygenase (12/15-LOX), (C) cyclooxygenase-1 (COX-1), and (D) cyclooxygenase-2 (COX-2) after two-week treatment with cannabidiol (CBD) in the SAT and VAT of rats fed a standard diet (Control) or high-fat diet (HFD). The total expression of the above proteins was standardized to the total protein expression, and the control group was set to 100%. The data are presented as the mean values \pm SD, $n=6$ in each group. * $p < 0.05$, significant difference: control group vs. experimental group; # $p < 0.05$, significant difference: HFD vs. experimental group.

(-36.7% , $p=0.0051$; Table 2), and IL-13 ($+894.8\%$, $p < 0.0001$; Table 2) compared with those in the standard rodent chow group. After HFD feeding, we observed altered concentrations of IL-7 (-37.9% , $p=0.0041$; Table 2), IL-10 (-35.2% , $p=0.0098$; Table 2), M-CSF ($+86.9\%$, $p=0.0011$; Table 2), and RANTES (-39.7% , $p=0.0018$; Table 2) in comparison with those in the control group. Moreover, in the HFD+CBD group, we detected elevated levels of G-CSF ($+42.0\%$, $p=0.0099$, vs. the control group; Table 2), GRO/KC ($+34.0\%$, $p=0.0003$, vs. the HFD; Table 2), IFN- γ ($+93.0\%$, $p < 0.0001$, vs. the control group; $+43.6\%$, $p=0.0021$, vs. the HFD group; Table 2), IL-4 ($+150.4\%$, $p < 0.0001$, vs. the control group; $+70.5\%$, $p=0.0081$, vs. the HFD group; Table 2), IL-5 ($+37.6\%$, $p=0.0004$, vs. the control group; Table 2), IL-6 ($+55.1\%$, $p=0.0085$, vs. the HFD group; Table 2), IL-13 ($+757.8\%$, $p < 0.0001$, vs. the control group; $+324.6\%$, $p < 0.0001$, vs. the HFD group; Table 2), and IL-17 A ($+43.2\%$, $p=0.0053$, vs. the control group; $+52.3\%$, $p=0.0008$, vs. the HFD group; Table 2), and M-CSF ($+204.4\%$, $p < 0.0001$, vs. the Control group; $+62.8\%$, $p=0.0041$, vs. the HFD group; Table 2). However, also in the HFD+CBD groups, we observed a substantial reduction in the concentrations of GM-CSF, IL-7, IL-10, RANTES, and TNF- α (-30.1% , $p=0.0196$; -53.1% , $p < 0.0001$; -51.2% , $p < 0.0001$; -32.1% , $p=0.0088$; and -27.0% , $p=0.0080$, respectively; Table 2) compared with those in the standard diet group.

Effects of two-week CBD treatment on histological changes in SAT and VAT

Quantitative (Table 3) and qualitative (Fig. 7) analyses of adipocyte circumference were performed by two experienced histologists (independent of each other). The measurements revealed a statistically significant increase in adipocyte size in both SAT and VAT in the group fed a HFD compared with those in the animals fed a standard diet ($+111.8\%$, $p=0.0246$; $+95.3\%$, $p=0.0004$, respectively; Table 3). The enlargement of adipocytes in both fat depots was observed in the group simultaneously treated with CBD and the HFD relative to the control group (SAT: $+142.1\%$, $p=0.0088$; VAT: $+79.1\%$, $p=0.0197$; Table 3). However, compared with those of the HFD group, the observed changes did not reach the level of significance after combined CBD and HFD treatment (SAT: $+14.3\%$, $p=0.5785$; VAT: -8.3% , $p=0.6100$; Table 3).

Discussion

The intracellular metabolism of adipocytes is highly important for the whole organism because of the storage of energy such as TAG, as well as the mobilization of energy reserves such as FFAs. White adipose tissue is

	Control	CBD	HFD	HFD + CBD
G-CSF	4.04 ± 1.19	2.26 ± 0.63 [*]	2.59 ± 0.62 [*]	2.14 ± 0.38 [*]
GM-CSF	110.46 ± 31.08	90.90 ± 23.32	148.39 ± 40.81	176.07 ± 53.14 [*]
GRO/KC	57.94 ± 10.51	71.93 ± 17.35	76.98 ± 19.26	71.66 ± 14.99
IFN- γ	195.22 ± 56.91	301.47 ± 82.82 [*]	370.24 ± 106.82 [*]	339.27 ± 79.19
IL-1 α	126.99 ± 31.12	81.99 ± 22.82	115.06 ± 34.00	170.57 ± 46.08 [#]
IL-1 β	141.40 ± 28.13	159.63 ± 39.59	146.89 ± 24.92	161.28 ± 37.16
IL-2	3959.27 ± 916.92	3672.89 ± 866.75	3582.71 ± 1032.73	2863.21 ± 750.80
IL-4	45.03 ± 8.03	41.42 ± 10.73	47.16 ± 11.95	75.83 ± 20.83 [#]
IL-5	519.63 ± 150.64	445.54 ± 97.89	458.44 ± 121.97	532.19 ± 130.26
IL-6	192.23 ± 52.57	236.24 ± 62.52	208.36 ± 37.53	252.38 ± 35.16
IL-7	294.23 ± 77.64	299.97 ± 61.45	368.22 ± 101.63	333.98 ± 94.93
IL-10	282.05 ± 72.86	250.01 ± 68.94	480.30 ± 125.32 [*]	325.50 ± 93.75 [#]
IL-12 p70	278.97 ± 63.01	221.09 ± 65.70	262.32 ± 78.28	401.16 ± 118.21 [#]
IL-13	342.43 ± 94.46	315.49 ± 94.03	193.93 ± 54.83 [*]	343.56 ± 89.33 [#]
IL-17 A	27.53 ± 7.74	41.55 ± 10.69	38.10 ± 10.91	35.60 ± 9.67
IL-18	1699.93 ± 411.30	1564.85 ± 352.14	1842.60 ± 468.56	665.49 ± 167.71 [#]
MCP-1	652.97 ± 186.58	842.22 ± 172.64	905.91 ± 262.04	1109.78 ± 323.09 [*]
M-CSF	5.79 ± 1.72	18.58 ± 4.15 [*]	9.50 ± 2.47	10.45 ± 2.83 [*]
MIP-1 α	12.22 ± 3.06	18.05 ± 3.83	17.87 ± 5.18	15.50 ± 4.08
MIP-3 α	34.53 ± 9.29	23.35 ± 6.05	26.76 ± 6.99	31.05 ± 9.29
RANTES	104.58 ± 25.39	67.61 ± 16.70	121.77 ± 34.84	136.93 ± 37.94
TNF- α	655.89 ± 171.52	705.59 ± 208.67	1154.47 ± 290.98 [*]	848.70 ± 215.44
VEGF	154.88 ± 43.36	328.61 ± 83.13 [*]	153.26 ± 42.65	288.82 ± 49.76 [#]

Table 1. The concentrations of selected cytokines, i.e., granulocyte colony-stimulating factor (G-CSF), granulocyte-macrophage colony-stimulating factor (GM-CSF), growth-regulated oncogene/keratinocyte chemoattractant (GRO/KC), Interleukin 1 α (IL-1 α), Interleukin 1 β (IL-1 β), Interleukin 2 (IL-2), Interleukin 4 (IL-4), Interleukin 5 (IL-5), Interleukin 6 (IL-6), Interleukin 7 (IL-7), Interleukin 10 (IL-10), Interleukin 12 p70 (IL-12 p70), Interleukin 13 (IL-13), Interleukin 17 A (IL-17 A), Interleukin 18 (IL-18), interferon γ (IFN- γ), macrophage inflammatory protein 1 α (MIP-1 α), and macrophage inflammatory protein 3 α (MIP-3 α), are regulated on activation, normal T-cell expressed and secreted (RANTES), tumor necrosis factor α (TNF- α), and vascular endothelial growth factor (VEGF) after two-week treatment with Cannabidiol (CBD) in the SAT of rats fed a standard diet (Control) or high-fat diet (HFD). The results are presented in picograms per milliliter of protein, $n = 10$ in each group. * $p < 0.05$, significant difference: control group vs. experimental group; # $p < 0.05$, significant difference: HFD vs. experimental group.

compartmentalized into two main depots, VAT and SAT, which differ in terms of morphology and functionality, including the secretion of adipokines and inflammatory cytokines or lipolysis rates³⁰. SAT fat depots, called metabolic “sinks” for excess lipid storage, constitute ~ 80% of the body fat in lean, healthy individuals and may have a more beneficial effect on whole-body lipid metabolism than VAT does³¹. VAT fat is highly metabolically active, and its excessive content, which is a main source of inflammatory cytokines, contributes to several conditions of metabolic syndrome³². Thus, understanding the early changes in these two types of adipose tissue that may be induced by phytocannabinoids is a promising future treatment. In this study, we focused on the effect of CBD on fat recomposition in obese adipose tissue during early-stage inflammation. In our study, obesity and early-stage inflammation were induced by a HFD, which was confirmed by increased deposition of the lipid precursor of inflammation, namely, AA, in the HFD group. In our previous paper on the same animal model, the induction of obesity was confirmed by increased body weight in HFD-fed animals²⁵. Unfortunately, CBD treatment in HFD-fed animals did not decrease body mass; thus, a more comprehensive analysis of CBD's effect on two adipose tissue depots seems to be reasonable.

Studies conducted by Silvestri et al. in an in vitro model of adipocytes and hepatocytes incubated with oleic acid revealed that CBD treatment decreased the accumulation of TAG in those cells¹⁴. These findings are only partially consistent with our study because we observed a decrease in TAG deposition only in VAT, without any changes in SAT. The other lipid fractions, namely, FFA and DAG, were decreased in both types of adipose tissue, which explains why some researchers noticed decreased levels of total fat after CBD treatment³³. Most importantly, CBD administered to HFD-fed rats lowered the level of PL, which is known to be the main source of AA, the lipid precursor of inflammation. Thus, the observed changes clearly showed that lowering the level of all the lipid fractions by CBD in more disease-susceptible VAT creates this phytocannabinoid, a substance that may improve excessive lipid deposition, a main factor in the development of metabolic complications. Although there was a significant decrease in lipid fraction deposition in both fat depots, histological studies revealed a similar direction of change, but the difference did not reach the level of significance. Thus, we may only speculate that longer CBD treatment may be needed for more pronounced changes, where the size of adipocytes in SAT

	Control	CBD	HFD	HFD + CBD
G-CSF	3.97 ± 1.16	3.86 ± 0.98	4.46 ± 1.26	5.65 ± 1.43 [*]
GM-CSF	157.58 ± 43.83	144.44 ± 34.10	132.26 ± 30.68	110.17 ± 30.57 [*]
GRO/KC	144.17 ± 39.44	158.69 ± 35.64	131.61 ± 21.27	176.31 ± 19.46 [#]
IFN- γ	447.45 ± 64.98	813.30 ± 203.61 [*]	601.32 ± 164.67	863.49 ± 139.07 ^{*#}
IL-1 α	200.65 ± 57.86	221.60 ± 59.42	247.30 ± 67.06	324.51 ± 57.77
IL-1 β	341.99 ± 96.14	335.97 ± 50.77	267.28 ± 59.58	299.83 ± 74.72
IL-2	5238.61 ± 1359.21	5004.37 ± 1424.89	4693.35 ± 651.90	5951.58 ± 1290.14
IL-4	109.73 ± 25.50	189.44 ± 52.49 [*]	161.19 ± 41.82	274.76 ± 76.76 ^{*#}
IL-5	608.28 ± 124.15	646.96 ± 133.58	706.31 ± 185.50	837.26 ± 109.72 [*]
IL-6	230.95 ± 64.04	408.99 ± 120.67 [*]	211.21 ± 57.74	327.64 ± 86.53 [#]
IL-7	757.13 ± 200.51	533.01 ± 157.69 [*]	470.10 ± 125.95 [*]	355.25 ± 80.83 [*]
IL-10	924.92 ± 274.61	585.18 ± 106.10 [*]	599.17 ± 154.56 [*]	451.06 ± 84.46 [*]
IL-12 p70	456.99 ± 117.47	441.05 ± 105.36	455.86 ± 80.03	574.98 ± 96.82
IL-13	162.27 ± 35.44	1614.25 ± 436.54 [*]	327.80 ± 91.80	1391.91 ± 266.27 ^{*#}
IL-17 A	53.58 ± 15.84	63.98 ± 14.67	50.38 ± 6.75	76.75 ± 16.85 ^{*#}
IL-18	1025.35 ± 273.62	1045.30 ± 296.91	1255.83 ± 334.75	876.06 ± 234.11
MCP-1	3709.34 ± 1030.66	3707.22 ± 1042.41	3017.24 ± 723.17	3134.47 ± 778.47
M-CSF	8.39 ± 2.35	10.35 ± 2.89	15.69 ± 3.84 [*]	25.55 ± 6.77 ^{*#}
MIP-1 α	52.67 ± 14.37	57.75 ± 16.05	52.13 ± 13.08	46.94 ± 11.93
MIP-3 α	45.78 ± 13.28	52.41 ± 13.45	42.48 ± 10.76	57.76 ± 8.14
RANTES	1304.84 ± 293.13	1265.40 ± 299.49	786.54 ± 179.70 [*]	885.39 ± 234.88 [*]
TNF- α	1442.95 ± 376.59	1171.35 ± 157.21	1173.40 ± 349.47	1053.75 ± 156.52 [*]
VEGF	192.88 ± 79.87	255.30 ± 40.59	142.59 ± 31.87	248.02 ± 74.58

Table 2. The concentrations of selected cytokines, i.e., granulocyte colony-stimulating factor (G-CSF), granulocyte-macrophage colony-stimulating factor (GM-CSF), growth-regulated oncogene/keratinocyte chemoattractant (GRO/KC), Interleukin 1 α (IL-1 α), Interleukin 1 β (IL-1 β), Interleukin 2 (IL-2), Interleukin 4 (IL-4), Interleukin 5 (IL-5), Interleukin 6 (IL-6), Interleukin 7 (IL-7), Interleukin 10 (IL-10), Interleukin 12 p70 (IL-12 p70), Interleukin 13 (IL-13), Interleukin 17 A (IL-17 A), Interleukin 18 (IL-18), interferon γ (IFN- γ), macrophage inflammatory protein 1 α (MIP-1 α), and macrophage inflammatory protein 3 α (MIP-3 α), are regulated on activation, normal T-cell expressed and secreted (RANTES), and tumor necrosis factor α (TNF- α) and vascular endothelial growth factor (VEGF) after two-week treatment with Cannabidiol (CBD) in the VAT of rats fed a standard diet (Control) or high-fat diet (HFD). The results are presented in picograms per milliliter of protein, $n = 10$ in each group. * $p < 0.05$, significant difference: control group vs. experimental group; # $p < 0.05$, significant difference: HFD vs. experimental group.

	Control	CBD	HFD	HFD + CBD
SAT	415.31 ± 217.91	664.98 ± 330.27	879.68 ± 371.11 [*]	1005.61 ± 388.33 [*]
VAT	960.22 ± 232.03	977.52 ± 296.93	1875.69 ± 355.32 [*]	1720.21 ± 630.02 [*]

Table 3. Morphometric analysis of adipocyte size in the VAT and SAT of rats fed a standard diet (control) or high-fat diet (HFD) after two weeks of Cannabidiol (CBD) treatment. The data are presented as the means ± standard deviations, $n = 6$ in each group. * $p < 0.05$, significant difference: control group vs. experimental group; # $p < 0.05$, significant difference: HFD vs. experimental group.

would be significantly increased. However, in VAT, only a slight decreasing tendency in the morphometric measurement of cell size in the HFD + CBD group was observed, which may be explained by the generation of new, small adipocytes.

However, AA derived from the PL fraction is also a precursor of two major endocannabinoids, anandamide (AEA) and 2-arachidonoylglycerol (2-AG), which belong to the N-acyl ethanolamines (NAEs) family and may be degraded by fatty acid amide hydrolase (FAAH) and monoacylglycerol lipase (MAGL), respectively, and are part of a large system known as the endocannabinoidome³⁴. CBD can interact with several molecular targets, including the endocannabinoidome, via direct and indirect mechanisms. CBD may act as an allosteric modulator of cannabinoid receptors (CB1, CB2), and through the inhibition of FAAH, it may increase the levels of the endogenous ligand AEA³⁵. As a result, CBD may enhance the anti-inflammatory effect of AEA³⁶. Moreover, the inhibition of FAAH and fatty acid-binding proteins (FABPs), which transport NAEs across the cell membrane to the intracellular FAAH enzyme for degradation, by CBD also causes the deposition of NAEs other than AEA, namely, palmitoylethanolamide (PEA) and oleoylethanolamide (OEA)^{37,38}. Studies conducted on diet-induced

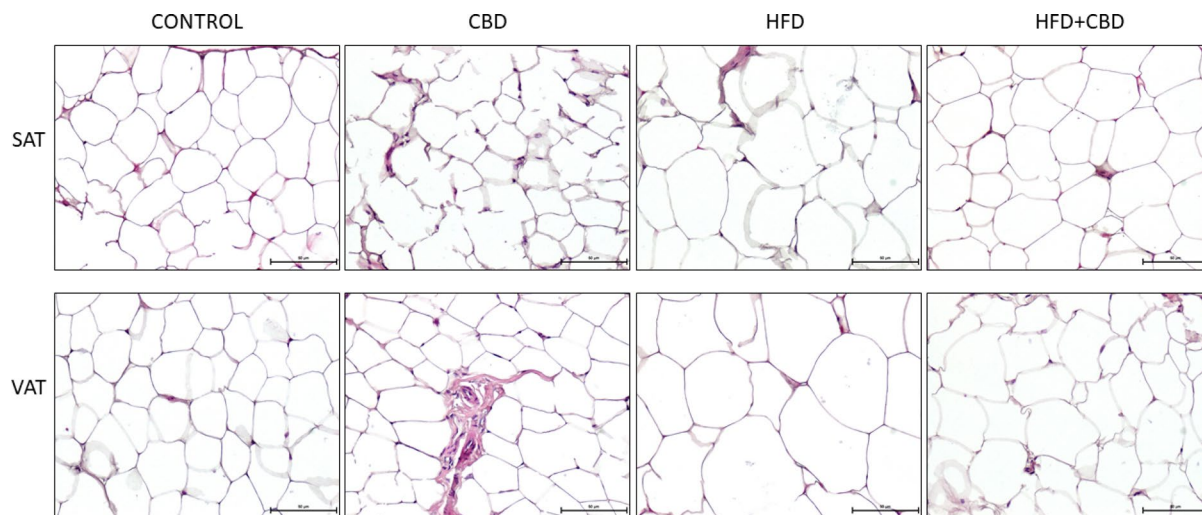


Fig. 7. Representative microphotographs of SAT and VAT after two weeks of cannabidiol (CBD) treatment in the SAT and VAT of rats fed a standard diet (control) or high-fat diet (HFD). The samples were stained with hematoxylin and eosin (H&E), $n = 6$ in each group. Images were taken at 200 \times magnification. Bars, 50 μ m, as indicated.

obese mice supplemented with OEA revealed decreased body mass, hepatic and body lipid accumulation, and diminished inflammation³⁹. Moreover, PEA, when administered to HFD-fed mice, reduced lipid deposition and insulin resistance in the liver, and in isolated form, the liver mitochondria also decreased oxidative stress⁴⁰. Thus, increased deposition of these NAEs by CBD may also be a way to exert beneficial effects under HFD conditions.

Although CBD has a low binding affinity for cannabinoid receptors, a main component of the endocannabinoidome, some desirable effects are observed through interactions with these receptors even at low concentrations⁴¹. The best example may be a study where chronic administration of low doses of CBD for 14 days decreased the body weight gain of rapidly growing male rats in a CB2-dependent manner³³. According to the cited literature, CBD's interaction with various molecular targets of the endocannabinoidome may explain the route by which CBD exerts its effects in our study.

In this study, we observed that under HFD conditions, CBD affects not only the content of accumulated lipid fractions but also their fatty acid compositions in two different manners depending on the type of fat depot. The increased availability of fatty acids in the diet is connected with disrupted intracellular lipid metabolism, i.e., with increased AA content in the PL of the adipocyte membrane⁴², which was also corroborated in our study in two types of fat depots. Notably, the elevated AA level induced by HFD was reduced by CBD treatment, both in SAT and VAT, in all the lipid fractions. The reduction in the level of AA, which acts as a trigger for an inflammatory response, may indicate the anti-inflammatory effect of CBD in adipose tissue. AA is metabolized into lipid proinflammatory molecules, i.e., prostaglandin series 2, *via* two isoforms of cyclooxygenase, COX-1 and COX-2⁴³. COX-1 is expressed constitutively in most tissues, including adipose tissue, whereas COX-2 expression is induced in an inflammatory state⁴⁴.

In line with previous reports conducted on white adipose tissue obtained from obese patients and on dietary and genetic models of obesity, we revealed significantly higher expression of both COX-1 and COX-2 in SAT and a trend toward an increase in VAT after HFD feeding^{45,46}. In VAT fat depots, CBD injection affected only COX-1, leading to a decrease in its expression. Interestingly, more pronounced alterations were observed in SAT, where CBD administration decreased the expression of both isoforms of COX in the CBD and HFD + CBD groups. This may point to the possible effectiveness of CBD against early-stage proinflammatory development, especially in SAT fat depots. Our observations are based on studies conducted on pharmacologically induced animal models of neuroinflammation as well as inflammation during endometriosis development, which showed that, in microglia and peritoneal fluids, CBD reduced elevated COX-2 expression driven by inflammation^{47,48}.

Products of lipoxygenase activity, especially the 12/15-lipoxygenase and 5-lipoxygenase pathways, play a role in the regulation of adipose tissue inflammation⁴⁹. Elevated 12/15-LOX gene expression in adipocytes and adipose tissue in obese Zucker rats was reported in a low-grade inflammatory state⁵⁰. In our research, we observed increased 12-/15-LOX protein expression in SATs derived from HFD-fed rats, which was considerably decreased after CBD administration. Although we observed increased expression of 12/15 LOX in VAT, it was not affected by a HFD alone. Thus, we speculate that the anti-inflammatory CBD effect is more pronounced in SAT, where inflammation further develops.

Polyunsaturated fatty acids (PUFAs) are key bioactive lipids that modulate the inflammatory response and the metabolism of adipose tissue⁵¹. PUFAs include two series of fatty acids: the n-6 and n-3 series. The n-6 PUFAs serve as precursors of inflammatory molecules. On the other hand, proresolving lipid mediators derived from n-3 PUFAs are involved in the resolution of adipose tissue inflammation and seem to have positive metabolic effects⁸. Thus, assessment of the changes in the n-3 and n-6 activity pathways induced by CBD in adipose tissue may reveal a lipid shift between proinflammatory n-6 fatty acids and inflammatory n-3 deposition. We

showed that this phytocannabinoid changed the concentration of PUFAs in both adipose tissue depots. In the SAT, CBD injected into HFD-fed rats did not affect the activity of the n-3 PUFA pathway, but it decreased the activity of n-6 in the DAG and PL fractions. Notably, the effect of CBD under conditions of overfeeding was more pronounced in VAT, where it led to an increase in n-3 and n-6 PUFA activity in the FFA fraction and, importantly, a significant decrease in n-6 activity in TAG and PL. On the basis of these findings, we may assume that the anti-inflammatory properties of CBD, expressed in the diminished activity of this pathway, which may lead to the production of proinflammatory mediators, are evident in both fat depots.

There is universal agreement that increased fat mass during obesity is associated with overproduction of proinflammatory cytokines and their secretion into the bloodstream in a depot-specific manner^{52,53}. In our study, HFD feeding caused an increase in the TNF α concentration only in the SAT, which is considered to be the main source of TNF α in obese individuals⁵². These findings may indicate early-stage inflammation in high-fat diet-fed rats. Interestingly, we observed a clear trend toward TNF α downregulation in these fat depots after CBD injection. Our observations are in line with reports summarized in a comprehensive review, which showed that CBD treatment reduces the tissue expression of TNF α , IL-6, and IL-1 β in various animal models of inflammation⁵⁴. At present, products that block proinflammatory cytokine release, known as TNF α inhibitors (such as infliximab), have been used in the clinic to treat more severe inflammatory conditions⁵⁵. However, its use may be associated with numerous side effects; thus, its use in low-grade inflammation is not possible. Therefore, natural substances that inhibit the expression of TNF α , such as CBD, may have therapeutic potential as supportive drugs for early-stage inflammatory treatment associated with obesity.

IFN- γ is another cytokine that seems to promote adipose tissue inflammation, and increased IFN- γ mRNA expression has been reported in the adipose tissue of obese animals and humans⁵⁶. Accordingly, we found that the IFN- γ protein concentration was increased in SAT and tended to increase in VAT derived from obese rats. Three animal studies confirmed that CBD administration attenuated plasma IFN- γ levels in nonobese animals^{57–59}. We revealed that CBD alone elevated the IFN- γ concentration in both fat deposits derived from normal chow-fed rats but that CBD alone had no significant effect on lipid overload conditions.

The increase in total macrophages and the increased ratio of M1- to M2-polarized macrophages are hallmarks of adipose tissue inflammation in obese individuals⁶⁰. M1 or “classically activated” macrophages are induced by proinflammatory mediators such as LPS and IFN- γ . M1 macrophages have increased proinflammatory molecule production, aggravating the inflammatory state. M2 or “alternatively activated” macrophages are promoted by IL-4, IL-13, and macrophage colony-stimulating factor (M-CSF)^{61,62}. Previous studies on experimental asthma in animal models have indicated that CBD reduces tissue and plasma levels of IL-4 and IL-13^{63,64}. Interestingly, CBD increased IL-4, IL-13, and M-CSF concentrations in VAT derived from HFD-fed rats, which seems to have benign effects, by promoting the anti-inflammatory phenotype of macrophages in adipose tissue during overfeeding. Another interleukin whose level is important in an inflammatory state is IL-10. However, reports regarding the effects of CBD on IL-10 expression are contradictory. Experiments in murine models of pharmacologically induced inflammation have shown that CBD increases anti-inflammatory IL-10 expression^{65,66}. Similarly, as shown by Britch et al., CBD administration reduces serum IL-10 levels in rats with persistent inflammatory pain⁵⁷. In contrast, an in vitro study conducted by Yeisley et al. revealed that CBD decreased the expression of IL-10 by lipopolysaccharide-activated macrophages⁶⁷. In the present study, we found that CBD administration significantly reduced IL-10 expression only in the SAT of rats receiving high-fat chow. It seems that different experimental models of inflammation may explain these discrepancies.

The data reported herein largely agree with other literature demonstrating the anti-inflammatory effects of CBD and provide preliminary evidence that potentially advantageous CBD influences lipid metabolism in the adipose tissue of obese animals in the context of diet-induced early-stage inflammation. Notably, although the anti-inflammatory effects of CBD are observed in both fat depots, lipid-lowering CBD activity varies across the analyzed tissues. In VAT, the observed diminished deposition of all the assessed lipid fractions may indicate that this adipose tissue may be more susceptible to the adiposity-lowering effect exerted by CBD, but longer exposure to this phytocannabinoid is likely needed to obtain visible changes in histology. Moreover, in VAT, beneficial changes in the composition of accumulated lipid precursors associated with inflammation caused by CBD are extremely valuable in the context of the pathophysiology of metabolic syndrome development. Although the SAT lipid-lowering effect was observed only in the FFA and DAG fractions, a decrease in AA deposition and a decrease in the n-6 activity pathway in the DAG and PL fractions without effects on n-3 indicate that this tissue responds less effectively to CBD treatment. Future studies are needed to elucidate the precise direct or indirect molecular mechanism by which CBD influences the inflammatory state in adipose tissues under conditions of lipid overload.

Data availability

The data presented in this study are available upon request from the corresponding author.

Received: 10 September 2025; Accepted: 14 January 2026

Published online: 22 January 2026

References

- Perchuk, A. et al. Developmental and behavioral effects in neonatal and adult mice following prenatal activation of endocannabinoid receptors by capsaicin. *Acta Pharmacol. Sin.* **40**, 418–424 (2019).
- Wellen, K. E. Inflammation, stress, and diabetes. *J. Clin. Invest.* **115**, 1111–1119 (2005).
- Chait, A. & den Hartigh, L. J. Adipose tissue Distribution, inflammation and its metabolic Consequences, including diabetes and cardiovascular disease. *Front. Cardiovasc. Med.* **7**, 7–22 (2020).
- Gregor, M. F. & Hotamisligil, G. S. Inflammatory mechanisms in obesity. *Annu. Rev. Immunol.* **29**, 415–445 (2011).

5. Maurizi, G., Della Guardia, L., Maurizi, A. & Poloni, A. Adipocytes properties and crosstalk with immune system in obesity-related inflammation. *J. Cell. Physiol.* **233**, 88–97 (2018).
6. Patterson, E., Wall, R., Fitzgerald, G. F., Ross, R. P. & Stanton, C. Health implications of high dietary omega-6 polyunsaturated Fatty acids. *J. Nutr. Metab.* **2012**, 539426. (2012).
7. Cole, B. K., Lieb, D. C., Dobrian, A. D. & Nadler, J. L. 12- and 15-lipoxygenases in adipose tissue inflammation. *Prostaglandins Other Lipid Mediat.* **104–105**, 84–92 (2013).
8. Masoodi, M., Kuda, O., Rossmeisl, M., Flachs, P. & Kopecky, J. Lipid signaling in adipose tissue: connecting inflammation & metabolism. *Biochim. Et Biophys. Acta (BBA) - Mol. Cell. Biology Lipids.* **1851**, 503–518 (2015).
9. Andre, C. M., Hausman, J. F. & Guerriero, G. Cannabis sativa: the plant of the thousand and one molecules. *Front. Plant. Sci.* **7**, 7–19 (2016).
10. Lucas, C. J., Galetti, P. & Schneider, J. The pharmacokinetics and the pharmacodynamics of cannabinoids. *Br. J. Clin. Pharmacol.* **84**, 2477–2482 (2018).
11. Shannon, S., Lewis, N., Lee, H. & Hughes, S. Cannabidiol in anxiety and sleep: A large case series. *Perm J.* **23**, 18–041 (2019).
12. Devinsky, O. et al. Cannabidiol: Pharmacology and potential therapeutic role in epilepsy and other neuropsychiatric disorders. *Epilepsia* **55**, 791–802 (2014).
13. Bielawiec, P., Harasim-Symbor, E., Chabowski, A. & Phytocannabinoids Useful drugs for the treatment of obesity? Special focus on Cannabidiol. *Front. Endocrinol. (Lausanne)*. **11**, 114 (2020).
14. Silvestri, C. et al. Two non-psychoactive cannabinoids reduce intracellular lipid levels and inhibit hepatosteatosis. *J. Hepatol.* **62**, 1382–1390 (2015).
15. Pellati, F. et al. Cannabis sativa L. and Nonpsychoactive Cannabinoids: Their Chemistry and Role against Oxidative Stress, Inflammation, and Cancer. *Biomed. Res. Int.* **2018**, 1–15. (2018).
16. Nagarkatti, P., Pandey, R., Rieder, S. A., Hegde, V. L. & Nagarkatti, M. Cannabinoids as novel Anti-Inflammatory drugs. *Future Med. Chem.* **1**, 1333–1349 (2009).
17. Rajesh, M. et al. Cannabidiol attenuates cardiac Dysfunction, oxidative Stress, Fibrosis, and inflammatory and cell death signaling pathways in diabetic cardiomyopathy. *J. Am. Coll. Cardiol.* **56**, 2115–2125 (2010).
18. Huang, Y. et al. Cannabidiol protects livers against nonalcoholic steatohepatitis induced by high-fat high cholesterol diet via regulating NF- κ B and NLRP3 inflammasome pathway. *J. Cell. Physiol.* **234**, 21224–21234 (2019).
19. Nowacki, D. et al. Lecithin derived from ω -3 PUFA fortified eggs decreases blood pressure in spontaneously hypertensive rats. *Sci. Rep.* **7**, 12373 (2017).
20. Zalewska, A., Maciejczyk, M., Szulimowska, J., Imierska, M. & Błachnio-Zabielska, A. High-Fat diet affects ceramide Content, disturbs mitochondrial redox Balance, and induces apoptosis in the submandibular glands of mice. *Biomolecules* **9**, 877 (2019).
21. Navarrete, F., Aracil-Fernández, A. & Manzanera, J. Cannabidiol regulates behavioural alterations and gene expression changes induced by spontaneous cannabinoid withdrawal. *Br. J. Pharmacol.* **175**, 2676–2688 (2018).
22. Merrick, J. et al. Identification of psychoactive degradants of Cannabidiol in simulated gastric and physiological fluid. *Cannabis Cannabinoid Res.* **1**, 102–112 (2016).
23. Hložek, T. et al. Pharmacokinetic and behavioural profile of THC, CBD, and THC + CBD combination after pulmonary, oral, and subcutaneous administration in rats and confirmation of conversion in vivo of CBD to THC. *Eur. Neuropsychopharmacol.* **27**, 1223–1237 (2017).
24. Nahler, G., Grotenhermen, F., Zuardi, A. W. & Crippa, J. A. S. A conversion of oral Cannabidiol to Delta9-Tetrahydrocannabinol seems not to occur in humans. *Cannabis Cannabinoid Res.* **2**, 81–86 (2017).
25. Charytoniuk, T. et al. Cannabidiol downregulates myocardial de Novo ceramide synthesis pathway in a rat model of High-Fat Diet-Induced obesity. *Int. J. Mol. Sci.* **23**, 2232 (2022).
26. Opęchowska, A. et al. Anti-inflammatory effects of Cannabidiol in early stages of neuroinflammation induced by high-fat diet in cerebral cortex of rats. *Toxicol. Appl. Pharmacol.* **484**, 116856 (2024).
27. Folch, J. & Lees, M. Sloane Stanley, G. H. A simple method for the isolation and purification of total lipides from animal tissues. *J. Biol. Chem.* **226**, 497–509 (1957).
28. Chabowski, A. et al. Fatty acid transporters involved in the palmitate and oleate induced insulin resistance in primary rat hepatocytes. *Acta Physiol. (Oxf)*. **207**, 346–357 (2013).
29. Konstanynowicz-Nowicka, K., Harasim, E., Baranowski, M. & Chabowski, A. New evidence for the role of ceramide in the development of hepatic insulin resistance. *PLoS One.* **10**, e0116858 (2015).
30. Rosen, E. D. & Spiegelman, B. M. What we talk about when we talk about fat. *Cell* **156**, 20–44 (2014).
31. Freedland, E. S. Role of a critical visceral adipose tissue threshold (CVATT) in metabolic syndrome: implications for controlling dietary carbohydrates: a review. *Nutr. Metab. (Lond)*. **1**, 12 (2004).
32. Lee, C. M. Y., Huxley, R. R., Wildman, R. P. & Woodward, M. Indices of abdominal obesity are better discriminators of cardiovascular risk factors than BMI: a meta-analysis. *J. Clin. Epidemiol.* **61**, 646–653 (2008).
33. Ignatowska-Jankowska, B., Jankowski, M. M. & Swiergiel, A. H. Cannabidiol decreases body weight gain in rats: involvement of CB2 receptors. *Neurosci. Lett.* **490**, 82–84 (2011).
34. Cristino, L., Bisogno, T. & Di Marzo, V. Cannabinoids and the expanded endocannabinoid system in neurological disorders. *Nat. Rev. Neurol.* **16**, 9–29 (2020).
35. Bisogno, T. et al. Molecular targets for Cannabidiol and its synthetic analogues: effect on vanilloid VR1 receptors and on the cellular uptake and enzymatic hydrolysis of Anandamide. *Br. J. Pharmacol.* **134**, 845–852 (2001).
36. Watanabe, K., Kayano, Y., Matsunaga, T., Yamamoto, I. & Yoshimura, H. Inhibition of Anandamide amidase activity in mouse brain microsomes by cannabinoids. *Biol. Pharm. Bull.* **19**, 1109–1111 (1996).
37. Elmes, M. W. et al. Fatty Acid-binding proteins (FABPs) are intracellular carriers for Δ 9-Tetrahydrocannabinol (THC) and Cannabidiol (CBD). *J. Biol. Chem.* **290**, 8711–8721 (2015).
38. Couttas, T. A. et al. Dose-dependent effects of oral Cannabidiol and delta-9-tetrahydrocannabinol on serum Anandamide and related N-acyl ethanolamines in healthy volunteers. *BMJ Mental Health.* **27**, 1–9 (2024).
39. Cimmino, F. et al. Anti-obesity effects of oleylethanolamide: modulation of mitochondrial bioenergetics, endocannabinoidome and gut Microbiome. *Biomed. Pharmacother.* **188**, 118201 (2025).
40. Annunziata, C. et al. Palmitoylethanolamide counteracts hepatic metabolic inflexibility modulating mitochondrial function and efficiency in diet-induced obese mice. *FASEB J.* **34**, 350–364 (2020).
41. Pertwee, R. G. Cannabinoid pharmacology: the first 66 years. *Br. J. Pharmacol.* **147**, 163–171 (2006).
42. Pietiläinen, K. H. et al. Association of lipidome remodeling in the adipocyte membrane with acquired obesity in humans. *PLoS Biol.* **9**, e1000623 (2011).
43. Smith, W. L., Urade, Y. & Jakobsson, P. J. Enzymes of the cyclooxygenase pathways of prostanoid biosynthesis. *Chem. Rev.* **111**, 5821–5865 (2011).
44. Fujimori, K. Prostaglandins as PPAR γ Modulators in Adipogenesis. *PPAR. Res.* **2012**, 1–8. (2012).
45. García-Alonso, V. et al. Prostaglandin E2 exerts multiple regulatory actions on human obese adipose tissue Remodeling, Inflammation, adaptive thermogenesis and lipolysis. *PLoS One.* **11**, e0153751 (2016).
46. Subbaramaiah, K. et al. Obesity is associated with inflammation and elevated aromatase expression in the mouse mammary gland. *Cancer Prev. Res. (Phila)*. **4**, 329–346 (2011).

47. Li, M. et al. Mitofusin 2 confers the suppression of microglial activation by cannabidiol: insights from in vitro and in vivo models. *Brain Behav. Immun.* **104**, 155–170 (2022).
48. Genovese, T. et al. Molecular and biochemical mechanism of Cannabidiol in the management of the inflammatory and oxidative processes associated with endometriosis. *Int. J. Mol. Sci.* **23**, 5427 (2022).
49. Horrillo, R. et al. 5-Lipoxygenase activating protein signals adipose tissue inflammation and lipid dysfunction in experimental obesity. *J. Immunol.* **184**, 3978–3987 (2010).
50. Chakrabarti, S. K. et al. Evidence for activation of inflammatory Lipoxygenase pathways in visceral adipose tissue of obese Zucker rats. *Am. J. Physiology-Endocrinology Metabolism.* **300**, E175–E187 (2011).
51. Calder, P. & Grimble, R. Polyunsaturated fatty acids, inflammation and immunity. *Eur. J. Clin. Nutr.* **56**, S14–S19 (2002).
52. Kern, P. A. et al. The expression of tumor necrosis factor in human adipose tissue. Regulation by obesity, weight loss, and relationship to lipoprotein lipase. *J. Clin. Invest.* **95**, 2111–2119 (1995).
53. Lee, M. & Fried, S. K. Depot-Specific biology of adipose tissues: links to fat distribution and metabolic risk. *Adipose Tissue Health Disease.* (Wiley), 283–306. <https://doi.org/10.1002/9783527629527.ch15> (2010).
54. Henshaw, F. R., Dewsbury, L. S., Lim, C. K. & Steiner, G. Z. The effects of cannabinoids on Pro- and Anti-Inflammatory cytokines: A systematic review of *In vivo* studies. *Cannabis Cannabinoid Res.* **6**, 177–195 (2021).
55. Lamb, C. A. et al. British society of gastroenterology consensus guidelines on the management of inflammatory bowel disease in adults. *Gut* **68**, s1–s106 (2019).
56. Rocha, V. Z. et al. Interferon- γ , a Th1 Cytokine, regulates fat inflammation. *Circ. Res.* **103**, 467–476 (2008).
57. Britch, S. C., Goodman, A. G., Wiley, J. L., Pondelick, A. M. & Craft, R. M. Antinociceptive and immune effects of Delta-9-Tetrahydrocannabinol or Cannabidiol in male versus female rats with persistent inflammatory pain. *J. Pharmacol. Exp. Ther.* **373**, 416–428 (2020).
58. Weiss, L. et al. Cannabidiol lowers incidence of diabetes in non-obese diabetic mice. *Autoimmunity* **39**, 143–151 (2006).
59. Elliott, D. M., Singh, N., Nagarkatti, M. & Nagarkatti, P. S. Cannabidiol attenuates experimental autoimmune encephalomyelitis model of multiple sclerosis through induction of Myeloid-Derived suppressor cells. *Front. Immunol.* **9**, 1782 (2018).
60. Lumeng, C. N., Bodzin, J. L. & Saltiel, A. R. Obesity induces a phenotypic switch in adipose tissue macrophage polarization. *J. Clin. Invest.* **117**, 175–184 (2007).
61. Gordon, S. Alternative activation of macrophages. *Nat. Rev. Immunol.* **3**, 23–35 (2003).
62. Zhou, D. et al. Macrophage polarization and function with emphasis on the evolving roles of coordinated regulation of cellular signaling pathways. *Cell. Signal.* **26**, 192–197 (2014).
63. Vuolo, F. et al. Evaluation of Serum Cytokines Levels and the Role of Cannabidiol Treatment in Animal Model of Asthma. *Mediators Inflamm.* **2015**, (2015).
64. Vuolo, F. et al. Cannabidiol reduces airway inflammation and fibrosis in experimental allergic asthma. *Eur. J. Pharmacol.* **843**, 251–259 (2019).
65. Borrelli, F. et al. Cannabidiol, a safe and non-psychotropic ingredient of the marijuana plant *cannabis sativa*, is protective in a murine model of colitis. *J. Mol. Med.* **87**, 1111–1121 (2009).
66. Verrico, C. D. et al. A randomized, double-blind, placebo-controlled study of daily Cannabidiol for the treatment of canine osteoarthritis pain. *Pain* **161**, 2191–2202 (2020).
67. Yeisley, D. J., Arabiyat, A. S. & Hahn, M. S. Cannabidiol-Driven alterations to inflammatory protein landscape of Lipopolysaccharide-Activated macrophages *In vitro* May be mediated by autophagy and oxidative stress. *Cannabis Cannabinoid Res.* **6**, 253–263 (2021).

Author contributions

Karolina Konstantynowicz-Nowicka: Conceptualization, Methodology, Data curation, Visualization, Investigation, Supervision, Writing-Reviewing and Editing; Klaudia Berk: Conceptualization, Writing-- Original draft preparation; Katarzyna Hodun: Software, Data curation; Algirdas Utkus: Writing-Reviewing and Editing, Data curation; Ewa Harasim-Symbor: Methodology, Investigation, Funding acquisition; Adrian Chabowski: Writing-Reviewing and Editing.

Funding

This work was supported by the National Science Centre of Poland (grant number: 2017/26/D/NZ3/01119) and the Medical University of Białystok (grant number: B.SUB.23.316).

Declarations

Competing interests

The authors declare no competing interests.

Ethics approval

All the experimental procedures were performed in accordance with the relevant guidelines and regulations. The animal experiments were conducted in accordance with the ARRIVE guidelines and were approved by the Animal Ethics Committee of Olsztyn (Approval No. 71/2018).

Additional information

Supplementary Information The online version contains supplementary material available at <https://doi.org/10.1038/s41598-026-36666-0>.

Correspondence and requests for materials should be addressed to K.K.-N.

Reprints and permissions information is available at www.nature.com/reprints.

Publisher's note Springer Nature remains neutral with regard to jurisdictional claims in published maps and institutional affiliations.

Open Access This article is licensed under a Creative Commons Attribution-NonCommercial-NoDerivatives 4.0 International License, which permits any non-commercial use, sharing, distribution and reproduction in any medium or format, as long as you give appropriate credit to the original author(s) and the source, provide a link to the Creative Commons licence, and indicate if you modified the licensed material. You do not have permission under this licence to share adapted material derived from this article or parts of it. The images or other third party material in this article are included in the article's Creative Commons licence, unless indicated otherwise in a credit line to the material. If material is not included in the article's Creative Commons licence and your intended use is not permitted by statutory regulation or exceeds the permitted use, you will need to obtain permission directly from the copyright holder. To view a copy of this licence, visit <http://creativecommons.org/licenses/by-nc-nd/4.0/>.

© The Author(s) 2026